

Tabular Two-Dimensional Correlation Analysis for Multifaceted Characterization Data

Shun Muroga^{1*}, Satoshi Yamazaki², Koji Michishio³, Hideaki Nakajima¹, Takahiro Morimoto¹, Nagayasu Oshima³, Kazufumi Kobashi¹, Toshiya Okazaki¹

1: Nano Carbon Device Research Center, National Institute of Advanced Industrial Science and Technology (AIST), Tsukuba Central 5, 1-1-1, Higashi, Tsukuba, Ibaraki 305-8565, Japan

2: Research Association of High-Throughput Design and Development for Advanced Functional Materials (ADMAT), Tsukuba, Ibaraki 305-8565, Japan

3: Research Institute for Measurement and Analytical Instrumentation, National Institute of Advanced Industrial Science and Technology (AIST), Tsukuba Central 2, 1-1-1, Umezono, Tsukuba, Ibaraki 305-8568, Japan

*Corresponding author: Shun Muroga, Nano Carbon Device Research Center, National Institute of Advanced Industrial Science and Technology (AIST), E-mail: muroga-sh@aist.go.jp

Keywords: tabular two-dimensional correlation analysis, multivariate statistics, multifaceted data, carbon nanotube

Abstract

We propose tabular two-dimensional correlation analysis for extracting features from multifaceted characterization data, essential for understanding material properties. This method visualizes similarities and phase lags in structural parameter changes through heatmaps, combining hierarchical clustering and asynchronous correlations. We applied the proposed method to datasets of carbon nanotube (CNTs) films annealed at various temperatures and revealed the complexity of their hierarchical structures, which include elements like voids, bundles, and amorphous carbon. Our analysis addresses the challenge of attempting to understand the sequence of structural changes, especially in multifaceted characterization data where 11 structural parameters derived from 8 characterization methods interact with complex behavior. The results show how phase lags (asynchronous changes from stimuli) and parameter similarities can illuminate the sequence of structural changes in materials, providing insights into phenomena like the removal of amorphous carbon and graphitization in annealed CNTs. This approach is beneficial even with limited data and holds promise for a wide range of material analyses, demonstrating its potential in elucidating complex material behaviors and properties.

Introduction

The materials that surround us exhibit hierarchical structures, with structural changes at each scale impacting the bulk properties. Analyzing such hierarchical structures at different length-scales is crucial for revealing the phenomena occurring in materials. For example, a comprehensive

understanding of polymeric materials, in principle, would require evaluations of structures spanning the chemical bonds to crystals, including primary repeating structures, molecular weight distribution, and lamellar structures formed by folded chains, and spherulites¹. This multifaceted analysis and unraveling of phenomena in materials is a universal practice, not limited to a specific material. However, multifaceted characterization data often contain changes where multiple factors exert complex effects in different sequences, making it challenging to arrive at a clear understanding through simple analysis. Consequently, there is a growing demand for analytical methods capable of effectively extracting information from multifaceted characterization data.

To establish methods for analyzing multifaceted characterization data, various approaches using data science have been pursued. One major obstacle that complicates analysis is multi-collinearity, where multiple factors change simultaneously, making it difficult to recognize behaviors by through visual inspection of the simple plotting of data. A typical approach to address such multi-collinearity is regression analysis that can recognize this such behavior. Partial least squares (PLS) regression is aptly suited for this task². PLS regression can be applied not only to commonly used vibrational spectroscopy data^{3,4} but also to multifaceted analytical data with strong multi-collinearity^{5,6}. For instance, applying PLS regression to a multifaceted dataset of carbon nanotube yarns has led to successful differentiation of contributions to mechanical strength and conductivity⁵. Additionally, recent advancements in deep learning and generative AI have enabled the development of multimodal deep learning, which integrates different types of multifaceted characterization data to predict material properties holistically⁷. These analytical methods are extremely effective in optimizing material properties, but challenges remain in understanding the sequence and impact of multiple factors affecting the multifaceted characterization data.

It is well known that two-dimensional correlation analysis is effective in evaluating the sequence of fluctuating factors from changes in analytical data. Especially due to its effectiveness in analyzing vibrational spectroscopy spectra and *in-situ* measured spectra, this method, also referred to as two-dimensional correlation spectroscopy (2DCOS), has been actively researched worldwide⁸⁻¹⁸. In 2DCOS, the extent and sequence of changes in absorption bands can be quantified by measuring the degree of change in sync (synchronous) or with a phase lag (asynchronous) in response to environmental or situational perturbations, such as temperature or strain. The use of synchronous and asynchronous spectra for feature extraction makes this method highly sensitive to detecting peak shifts or broadening due to interactions. In addition, its application has successful in analyzing phenomena, such as degradation¹⁹⁻²¹, curing reaction²², deformation of crystalline and amorphous regions^{23,24}, and interactions of proteins²⁵, moisture^{26,27}, polymers^{28,29}. Analytical methods have also evolved, including generalized two-dimensional correlation spectroscopy⁸, two-trace two-dimensional correlation spectroscopy (2T2D-COS) that extracts useful information from pairs of spectra^{15,22,26,30,31}, and disrelation mapping applied to hyperspectral imaging in pixel space^{28,32,33}. While 2DCOS is valuable

for deriving insights from one or two types of spectroscopic data obtained in response to perturbations, its application to three or more different types of multifaceted characterization data has been challenging.

In this study, we propose a general-purpose analytical method suitable for multifaceted characterization data: the tabular two-dimensional correlation analysis. This method is designed to quantitatively evaluate the similarity and sequence of changes using a table composed of multiple structural parameters obtained from various analytical techniques, not limited to spectroscopy. Specifically, the proposed analytical method involves rearranging structural parameters through hierarchical clustering^{4,7}, followed by calculating and visualizing their phase lags through asynchronous correlations in a heatmap format. This approach allows for a clear visualization of the degree of similarity and sequence among the changes in structural parameters. In this paper, we report on the application of the proposed method to two types of data: typical synthetic data and experimental data extracted from carbon nanotubes (CNTs) that have undergone annealing at high temperatures³⁴. Specifically, annealed CNT dataset includes 11 structural parameters measured by 8 different analytical techniques. This illustrates the versatility and effectiveness of the proposed method in handling complex multifaceted characterization datasets derived from a variety of analytical approaches.

Methods

Tabular two-dimensional correlation analysis

The proposed tabular two-dimensional correlation analysis comprises four steps: (1) normalization of each structural parameter to a range of 0-1, (2) sorting of structural parameters based on hierarchical clustering using cosine distance as a metric, (3) calculation of asynchronous correlations for each pair of structural parameters, and (4) creation of a dendrogram based on cosine distances and a heatmap where the values of asynchronous correlations are represented by pseudo-colors. Additionally, to validate the computational behavior, we used synthetic data consisting of 8 datasets, each generated by applying a different phase lag of $\pi/4$ to a sine function. This approach served as a test case to confirm the method's efficacy.

Annealed Carbon Nanotube Film Dataset

We utilized a dataset of CNT films annealed at high temperatures, previously reported using a multifaceted analytical approach³⁴. In this study, we compared the micro and macro structures using different analytical methods, focusing on a series of datasets comprising 8 methods and 11 structural parameters, described as scalar values (Table 1). This dataset involves films annealed under seven conditions (1200, 1600, 1800, 1900, 2000, 2200, and 2400°C) in a high-temperature furnace under an argon gas atmosphere, evaluated using 8 different measurement methods. The characteristics obtained from each measurement method are listed in the third column of Table 1. The data derived from these

measurements encompass a range of scales, including information about defects in the graphite structure, voids between tubes, the structure within and between bundles of multiple tubes, and impurities originating from amorphous carbon.

Table 1. Annealed CNT dataset composed of 11 structural parameters measured by 8 characterization methods.

Characterization Method	Structural Parameter	Description
Raman Spectroscopy ³⁵⁻³⁷	G/D band ratio	Indicator of carbon defects
X-ray Diffraction (XRD) ³⁸⁻⁴⁰	d_intertube(002)	Inter-tube spacing
	Lc_interlayer (004)	Crystallite size at inter-layer spacing
Wide Angle X-ray Scattering (WAXS) ^{41,42}	d(10)	(10) hexagonal closed packing of CNT bundles
	d(11)	(11) hexagonal closed packing of CNT bundles
Far-infrared (FIR) Spectroscopy ⁴³⁻⁴⁶	Effective length	Effective current path length between defects
Nitrogen Gas Adsorption ^{47,48}	Specific surface area	Overall specific surface area
	Adsorption amount at low pressure	Adsorption at interstitial sites in inter-tube spacing
X-ray Absorption Fine Structure (XAFS) ⁴⁹⁻⁵¹	π^*/σ^* band ratio	sp^2/sp^3 carbon ratio
Thermo-gravimetric Analysis (TGA) ⁵²	Weight loss at 500°C	Amount of carbonaceous impurity
Positron Annihilation ^{53,54}	Pore radius	Closed and open nano-spacing

Results and Discussion

The computational flow of the proposed tabular two-dimensional correlation analysis is illustrated in Fig 1. When handling multifaceted characterization data, several unique characteristics differentiate it from typical vibrational spectroscopy data. Firstly, multifaceted characterization data contains structural parameters with vastly different orders of magnitude and units, which, if untreated, could lead to biased data processing. To address this, we normalized each structural parameter to a range of 0 to 1. Next, we tackled the ordering of structural parameters. Unlike traditional vibrational spectroscopy data, structural parameters do not have a predefined sequence like wavelengths, wavenumbers, photon energy, etc. Therefore, we resolved this issue of sequence by sorting structural parameters based on hierarchical clustering, using multidimensional scaling, with cosine distance as one method for calculating similarities between parameters. Finally, we conducted two-dimensional correlation analysis, calculating asynchronous correlations for each pair of structural parameters. The values of asynchronous correlations were used as pseudo-colors to create a heatmap, and the distances

between pairs of structural parameters were visualized through a dendrogram. By implementing such a process, it becomes possible to conveniently determine the sequence of changes from asynchronous correlations while keeping high visibility of the similarity of parameters from adjacent positioning, useful for causal inference. This approach facilitates an intuitive understanding of how closely related parameters behave in relation to one another over the change of perturbation.

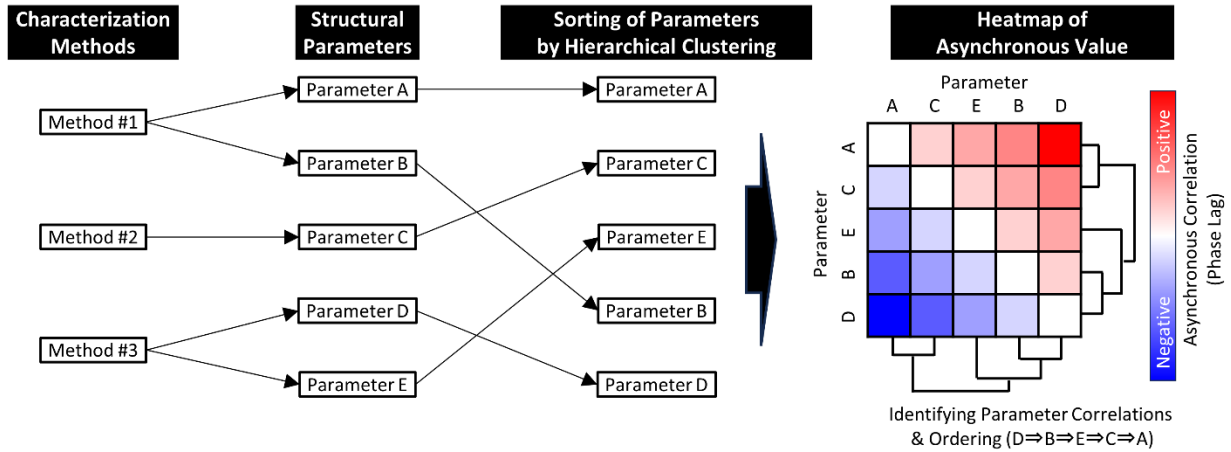


Figure 1. Schematic diagram of the proposed tabular two-dimensional correlation analysis.

The results of calculations performed using the proposed method, applied to a dataset simulating multifaceted characterization data obtained from experiments, are presented in Fig. 2. For validation, we artificially created functions based on the sine function, altering the phase by $\pi/4$ increments, resulting in eight data series labeled #1 to #8, representing perturbations ranging from 0 to 2π at 16 points (Fig. 2a). We then conducted hierarchical clustering on these data, with Fig. 2b showing a dendrogram representing the cosine distance differences. Adjacent IDs, i.e., synthetic data with small phase differences, are located in close proximity on the dendrogram, forming three major clusters: #1–3, 4–5, and 6–8. Based on these results, we sorted the synthetic data and calculated the asynchronous correlations for each pair, as shown in Fig. 2c. The heatmap reveals clear differences in the phases of the artificially created functions, for example, a significant phase lag between IDs #5 and 8. This demonstrates that our proposed analytical method successfully visualizes the similarity in parameter changes and phase delays.

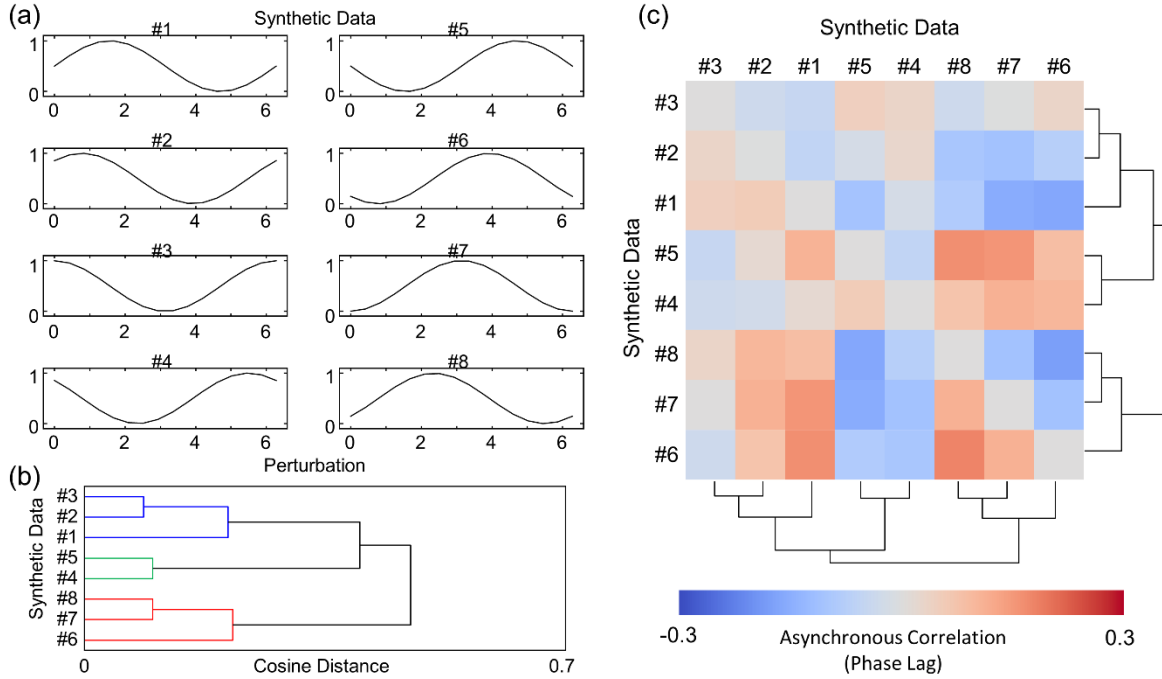


Figure 2. Tabular two-dimensional correlation analysis for synthetic data. (a) 8 synthetic data based on sine function. (b) Dendrogram of 8 synthetic data derived from hierarchical clustering. (c) Heatmap of asynchronous correlation of synthetic data.

Next, we examined the applicability of our proposed method to the carbon nanotube (CNT) data obtained from actual experiments (Fig. 3). CNTs, cylindrical materials made of carbon, possess outstanding mechanical, thermal, and electrical properties. In recent years, their application in transparent conductive films^{6,55}, supercapacitors^{56,57}, conductive fibers^{5,58–60}, and anti-static or reinforcement agents in rubber^{61–63} and plastics⁶⁴ have been anticipated. However, assemblies of CNTs are highly complex as they are comprised not only of carbon atoms but also a complex combination of hierarchical features as the length-scale increases, such as cylindrical tubes, bundling of multiple tubes, stacking structures, voids within and between tubes and bundles, tortuosity of these voids, carbon impurities, etc. Each of these features influence the properties observed at the macroscopic scale⁵². To understand the structural changes at these different levels, we annealed the CNTs under seven different temperature conditions and evaluated them using 8 analytical methods (Fig. 3a). Through this multifaceted analysis of annealed CNTs, we acquired 11 different structural parameters as outlined in Table 1³⁴. Applying the proposed tabular two-dimensional correlation analysis, we investigated the origins of structural changes occurring during high-temperature annealing.

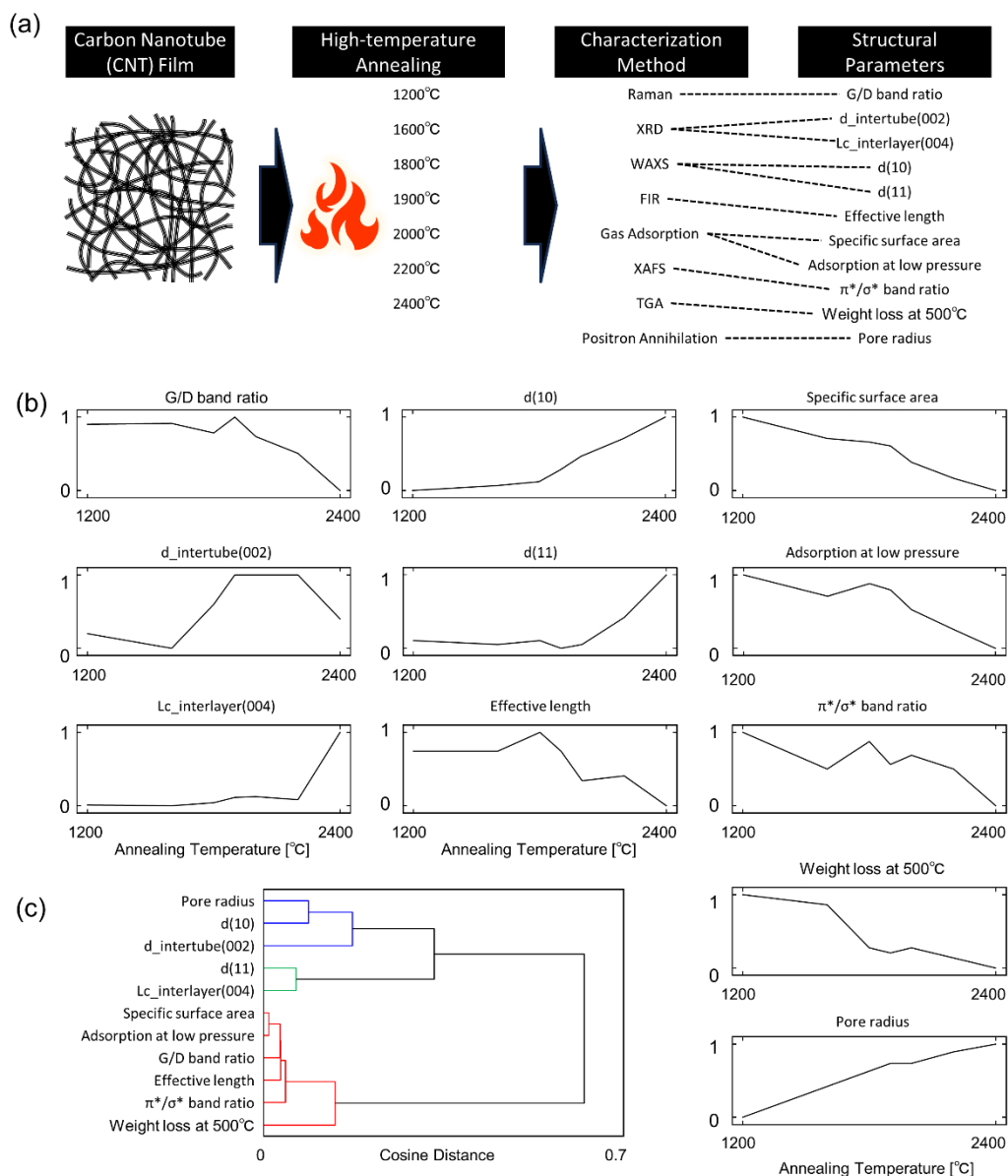


Figure 3. Carbon nanotube film (CNT) dataset with high-temperature annealing. (a) Schematic diagram of annealed CNT film dataset. (b) Effects of the perturbation (annealing temperature) on the 11 structural parameters of annealed CNT films. (c) Dendrogram of the 11 structural parameters in the annealed CNT film dataset, showing the similarity among the structural parameters.

The fluctuations of the 11 structural parameters with annealing temperature as the perturbation are shown in Fig. 3(b). The behavior of parameter changes varies across temperature ranges. For example, void sizes measured by positron annihilation spectroscopy show gradual changes, while parameters corresponding to the (004) interlayer diffraction observed by XRD, indicative of crystal size ($L_c_{\text{interlayer}}(004)$), undergo abrupt changes in the high-temperature range. These changes, which are complex behaviors, stem from different mechanisms and are difficult to comprehend and/or identify from a simple observation of a graph. To visualize these multiple structural parameter fluctuations, we

calculated cosine distances among structural parameters as a parameter similarity measure for hierarchical clustering analysis (Fig. 3(c)). Here, the parameters are broadly divided into three groups. The first cluster includes void size, the (10) plane diffraction related to the packing near the bundle, and the (002) plane diffraction corresponding to the distance between individual CNTs, parameters related to voids. The second cluster contains parameters related to crystal size and the (11) plane diffraction derived from packing at diagonal positions in the bundle, likely corresponding to structural changes accompanying crystal transformations. The third cluster encompasses numerous parameters, including those related to amorphous carbon and some pertaining to microstructure (corresponding to the pore volume) measured by gas adsorption, which are scattered near the cluster related to voids. Although these clusters roughly indicate groups of similar parameters, unraveling which structures change at what stages remains an extremely daunting challenge.

To visualize the pairwise relationships between parameters, we created a heatmap of asynchronous correlations using the proposed tabular two-dimensional correlation analysis in Fig. 4(a). Along with the parameter similarities shown in Fig. 3(c), the visualization of phase lags through asynchronous correlations allows for a discussion on the sequence of parameter changes. For instance, observing the top-right area of the heatmap, the asynchronous correlation between void size and the G/D band ratio takes a positive value, indicating a positive phase lag in the change of void size relative to the G/D band ratio. In other words, the change in void size occurs after the change in the G/D band ratio. By interpreting these asynchronous correlations, we organized the sequence of changes for each structural parameter relative to the annealing temperature (Fig. 4(b)). For example, the changes in parameters derived from thermogravimetric analysis and gas adsorption occurring earlier at lower temperatures suggest that the detachment of amorphous carbon precedes, influencing the sp^2/sp^3 carbon ratio and conductive paths. In the subsequent steps, the significant phase lags shown by XRD changes in the (10) and (11) planes suggest alterations in the voids between bundles and crystal size increase, likely due to increases in graphitization. This sequence of structural parameter changes indicates the interplay of two phenomena: the detachment of amorphous carbon and graphitization, thereby estimating the sequence of their impact. Thus, using our proposed method, we successfully extracted valuable information that aids in elucidating the mechanisms impacting microstructures during high-temperature annealing. While this analysis is feasible with a small amount of data, it is not universal but serves as a useful tool for generating insights for those with material knowledge, making it a promising approach in unraveling complex, multifaceted characterization data involving intricate phenomena.

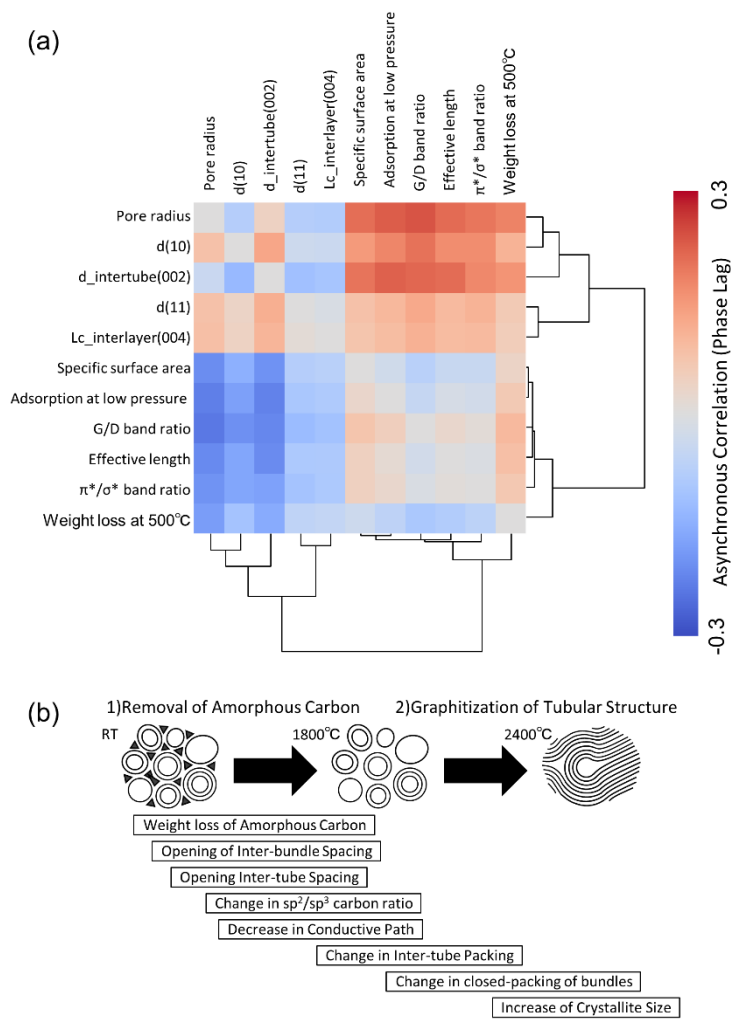


Figure 4. Effectivity and revealed mechanism of annealed CNT dataset based on the proposed method. (a) Heatmap of the asynchronous correlations of the structural parameters in annealed CNT dataset. (b) Mechanism of the high-temperature annealing of CNT derived from the similarities and the phase lags of the structural parameters.

Conclusion

We proposed tabular two-dimensional correlation analysis aimed at feature extraction from multifaceted characterization data. This method enables the clear visualization of the similarity in structural parameter changes and phase lags by constructing a heatmap that combines hierarchical clustering with asynchronous correlations of table data comprising different structural parameters. Applying this method to datasets of CNT films annealed at high temperatures, we obtained results that strongly support the understanding of structural origins due to differences in annealing temperatures. The proposed approach is effective even with a small amount of data, applicable to complex data where multiple mechanisms coexist, and aids in uncovering useful information for elucidating mechanisms. We are confident that this technique, while demonstrated on CNTs, can be expanded to a wide range

of material analyses.

Declaration of Conflicting Interests

The authors declared no potential conflicts of interest with respect to the research.

Funding

The authors disclosed receipt of the following financial support for the research: Japan Society for the Promotion of Science (JSPS) KAKENHI (No. JP22K04888, JP22K14571), a project (No. JPNP16010) commissioned by the New Energy and Industrial Technology Development Organization (NEDO), Nanotechnology Platform Program <Molecule and Material Synthesis> (JPMXP09S-16-SH-0027 & S-19-JI-0044) of the Ministry of Education, Culture, Sports, Science and Technology (MEXT).

Acknowledgments

We appreciate Dr. Ken Kokubo and Dr. Don N. Futaba for their support. The authors also thank Mr. Hikaru Yorozuya, Mrs. Yukari Urano, Mrs. Junko Kamata for help with experiments. We utilized a large language model for language polishing.

CRedit authorship contribution statement

Conceptualization: S.M., Methodology: S.M., Software: S.M., Formal Analysis: S.M., Investigation: S.M., S.Y., K.M., H. N., T.M., N.O., K.K., T.O., Visualization: S.M., K.K. Management: K.K., Supervision: T.O., Writing – Original Draft: S.M.

ORCID

Shun Muroga <https://orcid.org/0000-0002-6330-0436>

Koji Michishio <https://orcid.org/0000-0003-1381-7856>

Hideaki Nakajima <https://orcid.org/0000-0001-8678-0906>

Takahiro Morimoto <https://orcid.org/0000-0003-0439-7853>

Nagayasu Oshima <https://orcid.org/0000-0002-5713-112X>

Kazufumi Kobashi <https://orcid.org/0000-0002-7122-7638>

Toshiya Okazaki <https://orcid.org/0000-0002-5958-0148>

References:

1. E. Baer, A. Hiltner, H.D. Keith. “Hierarchical Structure in Polymeric Materials”. *Science*. 1987. 235(4792): 1015–1022. 10.1126/science.3823866.
2. D.M. Haaland, E.V. Thomas. “Partial least-squares methods for spectral analyses. 1. Relation to other quantitative calibration methods and the extraction of qualitative information”. *Anal. Chem*. 1988. 60(11): 1193–1202. 10.1021/ac00162a020.
3. S. Muroga, Y. Hikima, M. Ohshima. “Near-Infrared Spectroscopic Evaluation of the Water Content of Molded

- Poly lactide under the Effect of Crystallization”. *Appl Spectrosc.* 2017. 71(6): 1300–1309. 10.1177/0003702816681011.
4. S. Muroga, Y. Hikima, M. Ohshima. “Visualization of hydrolysis in polylactide using near-infrared hyperspectral imaging and chemometrics”. *J. Appl. Polym. Sci.* 2018. 135(8): 45898. 10.1002/app.45898.
 5. T. Watanabe, S. Yamazaki, S. Yamashita, T. Inaba, S. Muroga, T. Morimoto, et al. “Comprehensive Characterization of Structural, Electrical, and Mechanical Properties of Carbon Nanotube Yarns Produced by Various Spinning Methods”. *Nanomater.* 2022. 12(4): 593. 10.3390/nano12040593.
 6. Y. Nonoguchi, T. Miyao, C. Goto, T. Kawai, K. Funatsu. “Governing Factors for Carbon Nanotube Dispersion in Organic Solvents Estimated by Machine Learning”. *Adv. Mater. Inter.* 2022. 9(7): 2101723. 10.1002/admi.202101723.
 7. S. Muroga, Y. Miki, K. Hata. “A Comprehensive and Versatile Multimodal Deep-Learning Approach for Predicting Diverse Properties of Advanced Materials”. *Adv. Sci.* 2023. 10(24): 2302508. 10.1002/advs.202302508.
 8. I. Noda. “Generalized Two-Dimensional Correlation Method Applicable to Infrared, Raman, and other Types of Spectroscopy”. *Appl. Spectrosc.* 1993. 47(9): 1329–1336. 10.1366/0003702934067694.
 9. Y. Ozaki, Y. Liu, I. Noda. “Two-Dimensional Infrared and Near-Infrared Correlation Spectroscopy: Applications to Studies of Temperature-Dependent Spectral Variations of Self-Associated Molecules”. *Appl. Spectrosc.*, 1997. 51(4): 526–535. 10.1366/0003702971940521.
 10. I. Noda. “Determination of Two-Dimensional Correlation Spectra Using the Hilbert Transform”. *Appl. Spectrosc.* 2000. 54(7): 994–999. 10.1366/0003702001950472.
 11. Y. Mee Jung, I. Noda. “New Approaches to Generalized Two-Dimensional Correlation Spectroscopy and Its Applications”. *Appl. Spectrosc. Rev.* 2006. 41(5): 515–547. 10.1080/05704920600845868.
 12. I. Noda. “Two-dimensional codistribution spectroscopy to determine the sequential order of distributed presence of species”. *J. Mol. Struct.* 2014. 1069: 50–59. 10.1016/j.molstruc.2014.01.024.
 13. I. Noda. “Techniques useful in two-dimensional correlation and codistribution spectroscopy (2DCOS and 2DCDS) analyses”. *J. Mol. Struct.* 2016. 1124: 29–41. 10.1016/j.molstruc.2016.01.089.
 14. I. Noda. “Two-dimensional correlation analysis of spectra collected without knowing sampling order”. *J. Mol. Struct.* 2018. 1156: 418–423. 10.1016/j.molstruc.2017.11.085.
 15. I. Noda. “Two-trace two-dimensional (2T2D) correlation spectroscopy – A method for extracting useful information from a pair of spectra”. *J. Mol. Struct.* 2018. 1160: 471–478. 10.1016/j.molstruc.2018.01.091.
 16. A. He, Y. Zeng, X. Kang, S. Morita, Y. Xu, I. Noda, et al. “Novel Method of Constructing Two-Dimensional Correlation Spectroscopy without Subtracting a Reference Spectrum”. *J. Phys. Chem. A.* 2018. 122(3): 788–797. 10.1021/acs.jpca.7b10710.
 17. Y. Park, S. Jin, I. Noda, Y.M. Jung. “Recent progresses in two-dimensional correlation spectroscopy (2D-COS)”. *J. Mol. Struct.* 2018. 1168: 1–21. 10.1016/j.molstruc.2018.04.099.
 18. Y. Park, S. Jin, I. Noda, Y.M. Jung. “Emerging developments in two-dimensional correlation spectroscopy (2D-COS)”. *J. Mol. Struct.* 2020. 1217: 128405. 10.1016/j.molstruc.2020.128405.
 19. S. Yamane, H. Shinzawa, S. Ata, Y. Suzuki, A. Nishizawa, J. Mizukado. “A thermal oxidative degradation study

- of triallyl isocyanurate crosslinking moiety in fluorinated rubber by two-dimensional infrared correlation spectroscopy". *Vib. Spectrosc.* 2018. 98: 30–34. 10.1016/j.vibspec.2018.07.002.
20. S. Yamane, R. Watanabe, S. Ata, J. Mizukado, H. Shinzawa. "Solvent-induced degradation of polyurethane studied by two-dimensional (2D) infrared (IR) correlation spectroscopy". *Vib. Spectrosc.* 2020. 108: 103062. 10.1016/j.vibspec.2020.103062.
21. M. Koga, R. Watanabe, H. Hagihara, J. Mizukado, M. Tokita, H. Shinzawa. "Accelerated aging-induced variation of polypropylene (PP) structure studied by two-dimensional (2D) small-angle X-ray scattering (SAXS) correlation spectroscopy". *J. Mol. Struct.* 2020. 1207: 127764. 10.1016/j.molstruc.2020.127764.
22. T. Ishida, R. Watanabe, H. Shinzawa, J. Mizukado, H. Hagihara, R. Kitagaki, et al. "In-situ infrared cure monitoring combined with two-trace two-dimensional (2T2D) correlation analysis to elucidate the matrix–filler interaction of nanocomposites: Case of thermosetting urethane/silica nanospheres". *Polym. Test.* 2022. 112: 107587. 10.1016/j.polymertesting.2022.107587.
23. H. Shinzawa, J. Mizukado. "Rheo-optical two-dimensional (2D) near-infrared (NIR) correlation spectroscopy for probing strain-induced molecular chain deformation of annealed and quenched Nylon 6 films". *J. Mol. Struct.* 2018. 1158: 271–276. 10.1016/j.molstruc.2018.01.025.
24. M. Koga, M. Tokita, J. Mizukado, H. Shinzawa. "Two-dimensional (2D) small-angle X-ray scattering (SAXS) correlation spectroscopy for block copolymer consisting of microlamellar and liquid crystal (LC) structures". *J. Mol. Struct.* 2020. 1207: 127767. 10.1016/j.molstruc.2020.127767.
25. Y. Wu, L. Zhang, Y.M. Jung, Y. Ozaki. "Two-dimensional correlation spectroscopy in protein science, a summary for past 20 years". *Spectrochim. Acta A Mol. Biomol. Spectrosc.* 2018. 189: 291–299. 10.1016/j.saa.2017.08.014.
26. H. Shinzawa, J. Mizukado. "Water absorption by polyamide (PA) 6 studied with two-trace two-dimensional (2T2D) near-infrared (NIR) correlation spectroscopy". *J. Mol. Struct.* 2020. 1217: 128389. 10.1016/j.molstruc.2020.128389.
27. H. Asano, N. Ueno, Y. Ozaki, H. Sato. "Temperature-dependent structural variations of water and supercooled water and spectral analysis of Raman spectra of water in the OH-stretching band region and low-frequency region studied by two-dimensional correlation Raman spectroscopy -". *J. Raman Spectrosc.* 2022. 53(10): 1669. 10.1002/jrs.6444.
28. H. Lu, H. Shinzawa, S.G. Kazarian. "Intermolecular Interactions in the Polymer Blends Under High-Pressure CO₂ Studied Using Two-Dimensional Correlation Analysis and Two-Dimensional Disrelation Mapping". *Appl. Spectrosc.* 2021. 75(3): 250–258. 10.1177/0003702820978473.
29. D. Marlina, Y. Park, H. Hoshina, Y. Ozaki, Y.M. Jung, H. Sato. "A Study on Blend Ratio-dependent Far-IR and Low-frequency Raman Spectra and WAXD Patterns of Poly(3-hydroxybutyrate)/ poly(4-vinylphenol) Using Homospectral and Heterospectral Two-dimensional Correlation Spectroscopy". *Anal. Sci.* 2020. 36: 731–735. 10.2116/analsci.19P428.
30. S. Fujimoto, M. Aoyagi, H. Shinzawa. "Nanodiamond (ND)-based polyamide (PA) 66 nanocomposite studied with infrared (IR) microscopy and time-domain nuclear magnetic resonance (TD-NMR) combined with two-trace two-dimensional (2T2D) correlation analysis". *Spectrochim. Acta A Mol. Biomol. Spectrosc.* 2022. 280: 121572. 10.1016/j.saa.2022.121572.

31. R. Watanabe, A. Sugahara, H. Shinzawa, S. Yamane, S. Nakamura, H. Sato, et al. "Photodegradation behavior of polyethylene terephthalate analyzed by MALDI-TOFMS and ATR-FTIR microscopic analysis in combination with two-trace two-dimensional (2T2D) correlation mapping". *Polym. Degrad. Stab.* 2023. 208: 110246. 10.1016/j.polymdegradstab.2022.110246.
32. H. Shinzawa, J. Mizukado. "Near-infrared (NIR) disrelation mapping analysis for poly(lactic) acid nanocomposite". *Spectrochim. Acta A Mol. Biomol. Spectrosc.* 2017. 181: 1–6. 10.1016/j.saa.2017.03.026.
33. H. Shinzawa, H. Itasaka. "Glass fiber (GF)/polypropylene (PP) composite studied by Raman disrelation mapping". *Spectrochim. Acta A Mol. Biomol. Spectrosc.* 2022. 273: 121056. 10.1016/j.saa.2022.121056.
34. K. Kobashi, S. Yamazaki, K. Michishio, H. Nakajima, S. Muroga, T. Morimoto, et al. "Micro and macroscopic structure evolution of few-walled carbon nanotube bundled network by high temperature anneal". *Carbon.* 2023. 203: 785–800. 10.1016/j.carbon.2022.12.011.
35. F. Tuinstra, J.L. Koenig. "Raman Spectrum of Graphite". *J. Chem. Phys.* 1970. 53(3): 1126–1130. 10.1063/1.1674108.
36. E. Picheau, A. Impellizzeri, D. Rybkovskiy, M. Bayle, J.-Y. Mevellec, F. Hof, et al. "Intense Raman D Band without Disorder in Flattened Carbon Nanotubes". *ACS Nano.* 2021. 15(1): 596–603. 10.1021/acsnano.0c06048.
37. H. Nakajima, K. Kobashi, Y. Zhou, M. Zhang, T. Okazaki. "Quantitative analysis of the correlation between sp³ bonds and functional groups in covalently functionalized single-walled carbon nanotubes". *Carbon.* 2024. 216: 118495. 10.1016/j.carbon.2023.118495.
38. D.N. Futaba, K. Hata, T. Yamada, T. Hiraoka, Y. Hayamizu, Y. Kakudate, et al. "Shape-engineerable and highly densely packed single-walled carbon nanotubes and their application as super-capacitor electrodes". *Nature Mater.* 2006. 5(12): 987–994. 10.1038/nmat1782.
39. A. Milev, M. Wilson, G.S.K. Kannangara, N. Tran. "X-ray diffraction line profile analysis of nanocrystalline graphite". *Mater. Chem. Phys.* 2008. 111(2–3): 346–350. 10.1016/j.matchemphys.2008.04.024.
40. D.N. Futaba, T. Yamada, K. Kobashi, M. Yumura, K. Hata. "Macroscopic Wall Number Analysis of Single-Walled, Double-Walled, and Few-Walled Carbon Nanotubes by X-ray Diffraction". *J. Am. Chem. Soc.* 2011. 133(15): 5716–5719. 10.1021/ja2005994.
41. S. Rols, R. Almairac, L. Henrard, E. Anglaret, J.-L. Sauvajol. "Diffraction by finite-size crystalline bundles of single wall nanotubes". *Eur. Phys. J. B.* 1999. 10(2): 263–270. 10.1007/s100510050854.
42. J. Cambedouzou, M. Chorro, R. Almairac, L. Noé, E. Flahaut, S. Rols, et al. "X-ray diffraction as a tool for the determination of the structure of double-walled carbon nanotube batches". *Phys. Rev. B.* 2009. 79(19): 195423. 10.1103/PhysRevB.79.195423.
43. T. Morimoto, S.-K. Joung, T. Saito, D.N. Futaba, K. Hata, T. Okazaki. "Length-Dependent Plasmon Resonance in Single-Walled Carbon Nanotubes". *ACS Nano.* 2014. 8(10): 9897–9904. 10.1021/nn505430s.
44. T. Morimoto, T. Okazaki. "Optical resonance in far-infrared spectra of multiwalled carbon nanotubes". *Appl. Phys. Express.* 2015. 8(5): 055101. 10.7567/APEX.8.055101.
45. T. Morimoto, M. Ichida, Y. Ikemoto, T. Okazaki. "Temperature dependence of plasmon resonance in single-walled carbon nanotubes". *Phys. Rev. B.* 2016. 93(19): 195409. 10.1103/PhysRevB.93.195409.
46. T. Morimoto, K. Kobashi, T. Okazaki. "Carbon Nanotube Length Distribution Estimation by One-Dimensional

- Plasmon Resonance for Solid-State Samples”. *J. Phys. Chem. C*. 2021. 125(35): 19362–19367. 10.1021/acs.jpcc.1c04539.
47. K. Kobashi, H. Yoon, S. Ata, T. Yamada, D.N. Futaba, K. Hata. “Designing Neat and Composite Carbon Nanotube Materials by Porosimetric Characterization”. *Nanoscale Res Lett*. 2017. 12(1): 616. 10.1186/s11671-017-2384-2.
 48. K. Kobashi, Y. Iizumi, S. Muroga, T. Morimoto, T. Okazaki. “N₂ Gas Adsorption Sites of Single-Walled Carbon Nanotube Bundles: Identifying Interstitial Channels at Very Low Relative Pressure”. *Langmuir*. 2021. 37(30): 9144–9150. 10.1021/acs.langmuir.1c01248.
 49. K. Edamatsu, Y. Takata, T. Yokoyama, K. Seki, M. Tohnan, T. Okada, et al. “Local Structures of Carbon Thin Films Synthesized by the Hot Filament Chemical Vapor Deposition Method X-Ray-Absorption Near-Edge Structure and Raman Spectroscopic Studies”. *Jpn. J. Appl. Phys.* 1991. 30(5R): 1073. 10.1143/JJAP.30.1073.
 50. M. Imamura, H. Shimada, H. Matsubayashi, M. Yumura, K. Uchida, S. Oshima, et al. “XANES study on the electronic states of carbon nanotube and related materials”. *Physica B: Condens. Matter*. 1995. 208–209: 541–542. 10.1016/0921-4526(94)00744-G.
 51. I. Jimenez, R. Gago, J.M. Albella. “Fine structure at the X-ray absorption π^* and σ^* bands of amorphous carbon”. *Diam. Relat. Mater.* 2003. 12(2): 110–115. 10.1016/S0925-9635(03)00011-6.
 52. K. Kobashi, S. Ata, T. Yamada, D.N. Futaba, T. Okazaki, K. Hata. “Classification of Commercialized Carbon Nanotubes into Three General Categories as a Guide for Applications”. *ACS Appl. Nano Mater.* 2019. 2(7): 4043–4047. 10.1021/acsanm.9b00941.
 53. J.V. Olsen, P. Kirkegaard, N.J. Pedersen, M. Eldrup. “PALSfit: A new program for the evaluation of positron lifetime spectra”. *Phys. Status Solidi (c)*. 2007. 4(10): 4004–4006. 10.1002/pssc.200675868.
 54. B.E. O’Rourke, N. Oshima, A. Kinomura, R. Suzuki. “Development of a vertical slow positron beamline at AIST”. *JJAP Conference Proceedings*. 2014. 2: 011304–011304. 10.56646/jjapcp.2.0_011304.
 55. Y. Zhou, R. Azumi, S. Shimada. “A highly durable, stretchable, transparent and conductive carbon nanotube–polymeric acid hybrid film”. *Nanoscale*. 2019. 11(9): 3804–3813. 10.1039/C8NR08399A.
 56. T. Honda, S. Muroga, H. Nakajima, T. Shimizu, K. Kobashi, H. Morita, et al. “Virtual experimentations by deep learning on tangible materials”. *Commun. Mater.* 2021. 2(1): 88. 10.1038/s43246-021-00195-2.
 57. T. Shimizu, K. Kobashi, H. Nakajima, S. Muroga, T. Yamada, T. Okazaki, et al. “Supercapacitor Electrodes of Blended Carbon Nanotubes with Diverse Conductive Porous Structures Enabling High Charge/Discharge Rates”. *ACS Appl. Energy Mater.* 2021. 4(9): 9712–9720. 10.1021/acsaem.1c01802.
 58. X. Wu, T. Morimoto, K. Mukai, K. Asaka, T. Okazaki. “Relationship between Mechanical and Electrical Properties of Continuous Polymer-Free Carbon Nanotube Fibers by Wet-Spinning Method and Nanotube-Length Estimated by Far-Infrared Spectroscopy”. *J. Phys. Chem. C*. 2016. 120(36): 20419–20427. 10.1021/acs.jpcc.6b06746.
 59. X. Wu, K. Mukai, K. Asaka, T. Morimoto, T. Okazaki. “Effect of surfactants and dispersion methods on properties of single-walled carbon nanotube fibers formed by wet-spinning”. *Appl. Phys. Express*. 2017. 10(5): 055101. 10.7567/APEX.10.055101.
 60. N. Tajima, T. Watanabe, T. Morimoto, K. Kobashi, K. Mukai, K. Asaka, et al. “Nanotube length and density

- dependences of electrical and mechanical properties of carbon nanotube fibres made by wet spinning”. *Carbon*. 2019. 152: 1–6. 10.1016/j.carbon.2019.05.062.
61. K. Kobashi, A. Sekiguchi, T. Yamada, S. Muroga, T. Okazaki. “Dispersions of High-Quality Carbon Nanotubes with Narrow Aggregate Size Distributions by Viscous Liquid for Conducting Polymer Composites”. *ACS Appl. Nano Mater.* 2020. 3(2): 1391–1399. 10.1021/acsanm.9b02252.
62. S. Muroga, Y. Takahashi, Y. Hikima, S. Ata, M. Ohshima, T. Okazaki, et al. “New evaluation method for the curing degree of rubber and its nanocomposites using ATR-FTIR spectroscopy”. *Polym. Test.* 2021. 93: 106993. 10.1016/j.polymertesting.2020.106993.
63. S. Muroga, Y. Takahashi, Y. Hikima, S. Ata, S.G. Kazarian, M. Ohshima, et al. “Novel Approaches to In-Situ ATR-FTIR Spectroscopy and Spectroscopic Imaging for Real-Time Simultaneous Monitoring Curing Reaction and Diffusion of the Curing Agent at Rubber Nanocomposite Surface”. *Polymers*. 2021. 13(17): 2879. 10.3390/polym13172879.
64. Muroga S., Miki Y., Kishi R., Tomonoh S., Kokubo K., Okazaki T., et al. “Fabrication and Characterization of Highly Tough Multi-wall CNT/PEEK Nanocomposites”. *Seikei-Kakou*. 2021. 33(12): 438–440. 10.4325/seikeikakou.33.438.